

U.S. DEPARTMENT OF COMMERCE  
National Technical Information Service

AD-A027 029

USE OF PHASE-CHANGE PAINTS TO STUDY FIN-BODY  
INTERFERENCE HEATING

NAVAL SURFACE WEAPONS CENTER

1 APRIL 1976

204091

**NSWC/WOL/TR 75-62**

**NSWC/WOL/TR 75-62**

# NSWC

## **TECHNICAL REPORT**

**WHITE OAK LABORATORY**

**USE OF PHASE-CHANGE PAINTS TO STUDY FIN-BODY INTERFERENCE HEATING**

BY  
Joseph D. Gillerlain, Jr.

1 APRIL 1976

NAVAL SURFACE WEAPONS CENTER  
WHITE OAK LABORATORY  
SILVER SPRING, MARYLAND 20910

- Approved for public release; distribution unlimited.

**NAVAL SURFACE WEAPONS CENTER  
WHITE OAK, SILVER SPRING, MARYLAND 20910**

REPRODUCED BY  
NATIONAL TECHNICAL  
INFORMATION SERVICE  
U. S. DEPARTMENT OF COMMERCE  
SPRINGFIELD, VA. 22161

JUN 21 1976

## UNCLASSIFIED

SECURITY CLASSIFICATION OF THIS PAGE (When Data Entered)

REPORT DOCUMENTATION PAGE		READ INSTRUCTIONS BEFORE COMPLETING FORM
1. REPORT NUMBER NSWC/WOL/TR 75-62	2. GOVT ACCESSION NO.	3. RECIPIENT'S CATALOG NUMBER
4. TITLE (and Subtitle)  Use of Phase-Change Paints to Study Fin-Body Interference Heating		5. TYPE OF REPORT & PERIOD COVERED
		6. PERFORMING ORG. REPORT NUMBER
7. AUTHOR(s)  Joseph D. Gillerlain, Jr.		8. CONTRACT OR GRANT NUMBER(s)
9. PERFORMING ORGANIZATION NAME AND ADDRESS  Naval Surface Weapons Center White Oak Laboratory Silver Spring, Maryland 20910		10. PROGRAM ELEMENT, PROJECT, TASK AREA & WORK UNIT NUMBERS  A320-320C/WF32-322-205
11. CONTROLLING OFFICE NAME AND ADDRESS		12. REPORT DATE  1 April 1976
		13. NUMBER OF PAGES  38
14. MONITORING AGENCY NAME & ADDRESS (if different from Controlling Office)		15. SECURITY CLASS. (of this report)  UNCLASSIFIED
		15a. DECLASSIFICATION/DOWNGRADING SCHEDULE
16. DISTRIBUTION STATEMENT (of this Report)  Approved for public release; distribution unlimited.		
17. DISTRIBUTION STATEMENT (of the abstract entered in Block 20, if different from Report)		
18. SUPPLEMENTARY NOTES  Excerpts presented at the Tenth Navy Symposium on Aeroballistics 15-17 July 1975, Fredericksburg, Virginia		
19. KEY WORDS (Continue on reverse side if necessary and identify by block number) Temperature-sensitive paints Phase-change paints Interference heating Fin-body interference		
20. ABSTRACT (Continue on reverse side if necessary and identify by block number)  In recent years the phase-change paint technique has evolved into an accepted diagnostic tool in high-speed wind-tunnel testing. The method is considered capable of providing reliable quantita- tive heat-transfer results for complex configurations with interference heating patterns of unknown extent and location. This report documents use of the method at the Naval Surface Weapons Center, White Oak Laboratory, to study aerodynamic		

UNCLASSIFIED

SECURITY CLASSIFICATION OF THIS PAGE(When Data Entered)

interference heating on fin-body configurations. Various aspects of both the underlying theory and the experimental method are enumerated based on experience and on information from other researchers. Analytic relationships are presented which indicate how uncertainties in the various input parameters affect the uncertainty in the heat-transfer coefficient. Advantages and disadvantages of the phase-change paint method are discussed.

NSWC/WOL/TR 75-62

1 April 1976

USE OF PHASE-CHANGE PAINTS TO STUDY FIN-BODY INTERFERENCE HEATING

This report documents use of the phase-change paint technique at the Naval Surface Weapons Center, White Oak Laboratory, to study aerodynamic interference heating on fin-cone configurations. Theoretical and experimental aspects of the method are discussed.

This project was performed for the Naval Air Systems Command under AIRTASK Number A320-320C/WF32-322-205.

The author acknowledges the assistance of personnel in the Experimental Aerodynamics and the Facility Engineering Support Branches in performing these tests and in preparing this report. Special thanks go to Mr. Robert G. Ball for his photographic expertise.

*R. W. Schlie*

R. W. SCHLIE  
By direction

## CONTENTS

	Page
INTRODUCTION .....	5
BACKGROUND .....	6
THEORY .....	7
EXPERIMENTAL TECHNIQUE .....	8
Choice of Model Material .....	8
Model Configuration for Fin-Body Interference Heating Tests ..	10
Phase-Change Coatings .....	10
Data Acquisition .....	10
Photographic Conditions .....	11
EXPERIMENTAL RESULTS .....	11
Data Reduction .....	11
Isoheating Contours .....	11
UNCERTAINTY IN HEAT-TRANSFER COEFFICIENT .....	12
Validity of Semi-Infinite Slab Assumption .....	12
Sensitivity to Thermophysical Properties and Initial Time ...	12
Sensitivity to Errors in Temperature Inputs .....	13
Sensitivity to Error in Adiabatic Wall Temperature .....	14
Sensitivity to Error in Initial Model Temperature .....	14
Sensitivity to Error in Melt Temperature of Phase-Change Coating .....	14
General Comments .....	15
CONCLUSIONS .....	15
APPENDIX A .....	A-1
APPENDIX B .....	B-1

## TABLES

Table	Title	
1	Thermophysical Properties of Teflon .....	17
A-1	Phase-Change Paint Calibration Results .....	A-2

## ILLUSTRATIONS

Figure	Title	
1	Solution of One-Dimensional Heat Conduction Equation ..	18
2	Teflon Heat-Transfer Model .....	19
3	Schematic Diagram of Fin-Cone Model .....	20
4	Schematic Diagram of Finned Extension .....	21
5	Schematic Diagram of Test Setup .....	22
6	Isoheating Contours for Flush-Mounted Unswept Fin - Side View .....	23
7	Isoheating Contours for Flush-Mounted Unswept Fin - Top View .....	24
8	Isoheating Contours for Flush-Mounted 60°-Swept Fin - Side View .....	25

## ILLUSTRATIONS (Cont'd)

Figure	Title	Page
9	Isoheating Contours for Flush-Mounted 60°-Swept Fin - Top View .....	26
10	Error in Heat-Transfer Coefficient Due to Uncertainty in Initial Time of Exposure to Flow .....	27
11	Error in Heat-Transfer Coefficient Due to Uncertainty in Adiabatic Wall Temperature .....	28
12	Error in Heat-Transfer Coefficient Due to Uncertainty in Initial Model Temperature .....	29
13	Error in Heat-Transfer Coefficient Due to Uncertainty in Phase-Change Paint Melt Temperature .....	30
A-1	Schematic Diagram of Temperature-Sensitive Paint Calibration Setup .....	A-3

## SYMBOLS

$C_p$	specific heat of model material
$h$	heat-transfer coefficient
$k$	thermal conductivity of model material
$l$	characteristic depth into model
$t$	time
$t_d$	thermal diffusion time
$x$	depth into model material normal to surface
$R_c$	radius of curvature of model surface
$T$	temperature
$T_{aw}$	adiabatic wall temperature on model
$T_i$	initial temperature of model
$T_m$	melt temperature of phase-change coating
$\alpha$	thermal diffusivity
$\beta$	dimensionless parameter (Eq. (8))
$\rho$	density of model material
$\Gamma(\beta)$	dimensionless common factor (Eq. (16))



## INTRODUCTION

In recent years a number of thermal mapping techniques have evolved into accepted diagnostic tools to study problems in aerodynamic heating. This report deals with the so-called phase-change paint technique, which employs temperature-sensitive coatings which change phase, i.e., melt, from an opaque crystalline solid to a clear liquid at a specified temperature. The method was pioneered by Jones and Hunt<sup>(1)</sup> at NASA, Langley Research Center, in the mid-sixties. Since then, the technique has been used at most major wind-tunnel facilities. (See Refs. (2) and (3), for example.)

Initially, the phase-change paint method was recognized as one which provided only a qualitative look at aeroheating patterns on complex geometries. Two strong points of the method were (1) that the models were generally easy to fabricate, since no extensive instrumentation was required, and (2) that these models were essentially fully "instrumented" for situations where the interference heating patterns were of unknown location and extent. The phase-change paint technique has since developed to the point that one may expect to obtain reliable quantitative data in good agreement with heat-transfer results from methods employing thermocouples or heat-flux gages, for example.

Almost every user of the phase-change paint technique generally has seen fit to document his results and to comment on certain aspects of the method. In this respect, this report is similar to others in the literature. It documents the use of the phase-change paint technique at the Naval Surface Weapons Center, White Oak Laboratory, to study aerodynamic interference heating problems on fin-body configurations. It addresses various features of the paint method and presents some representative test results. A subsequent technical report documents in more detail the results of a fin-cone interference heating investigation<sup>(4)</sup>.

- 
- (1) Jones, R. A., and Hunt, J. L., "Use of Fusible Temperature Indicators for Obtaining Quantitative Aerodynamic Heat-Transfer Data," NASA TR R-230, Feb 1966
- (2) Martindale, W. R., "Interference Heating Measurements on a Hypersonic Cruise Vehicle Wing Using the Phase-Change Paint Technique," AEDC-TR-70-78, Apr 1970
- (3) Patterson, J. L., "Heat Transfer Testing in the AFFDL High Temperature Facility Using the Phase Change Coating Technique," AFFDL FXG TM 70-12, Aug 1970
- (4) Gillerlain, J. D., Jr., "Experimental Investigation of a Fin-Cone Interference Flow Field at Mach 5," NSWC/WOL/TR 75-63

This report elaborates on certain points of both the underlying theory and the experimental technique in an effort to provide an overview of the phase-change paint technique. As contributions to the theory behind the method, analytic relationships have been worked out which indicate what relative uncertainty in the heat-transfer coefficient (as determined from reduction of the phase-change paint data) is produced by uncertainties in the various input parameters relevant to the problem. This information should provide future users of the method with helpful guidelines in designing experiments.

## BACKGROUND

Two common types of temperature-sensitive coatings are available commercially. Each indicates surface temperature by a different observable mechanism. One type is a so-called color-change coating (known as Detectotemp) which exhibits a specified color change or series of color changes over a specified temperature range. The second type is a phase-change coating (called Tempilaq) which melts irreversibly from an opaque crystalline solid to a clear liquid at a single specified temperature. A bench-test program on these two types of coatings was carried out. Based on results of these tests, and on results reported by other researchers, the phase-change paints were selected over the color-change paints as being better suited for use in a short-duration high-speed wind-tunnel facility. A series of calibration checks involving both types of coatings further reinforced the choice of Tempilaq for our purposes. These calibration checks are included as Appendix A. Briefly, it was found that Detectotemp color-change coatings have a built-in time-temperature history associated with their specified color changes. If the color change occurs in a very short time period (less than 30 minutes), as is usually the case in high-speed wind-tunnel tests, then the temperature at the instant of the color change is higher than the rated temperature. The manufacturer of Detectotemp provides a brochure<sup>(5)</sup> which contains calibration charts of color-change temperature versus heating time. In addition, these coatings may be subject to extraneous color changes as the result of loss of evaporative salts when a vacuum is drawn on the wind-tunnel test cell.

The phase-change paints are considered to be more reliable temperature indicators for use in short-duration (with a lower limit of test times greater than about two seconds for reasons to be seen later) high-speed wind-tunnel tests. They are not known to vary with either pressure or heating rate in melting at their rated temperature<sup>(1)</sup>. Moreover, they do not involve the subjective element of color discrimination, the melt process being one of an opaque solid turning to a clear liquid.

---

<sup>(5)</sup> Thermochrom and Detectotemp Information Brochure, published by H. V. Hardman Co., Inc., Belleville, New Jersey

## THEORY

Reduction of the phase-change paint heat-transfer data is based on solving the transient, one-dimensional heat-conduction equation given by

$$\frac{\partial T}{\partial t} = \frac{k}{\rho C_p} \frac{\partial^2 T}{\partial x^2} \quad (1)$$

where  $T$  is temperature,  $t$  is time,  $x$  is distance normal from the surface into the model, and  $k$ ,  $\rho$ , and  $C_p$  are the thermal conductivity, the density and the specific heat of the model material, respectively. The mathematical boundary conditions and assumptions necessary to solve Equation (1) may be stated in the following physical terms:

1. The model is initially, at a uniform temperature,

$$T(x,0) = T_i \quad (2)$$

2. The depth of heat penetration into the model is small compared to the wall thickness and surface radius of curvature,

$$T(\infty, t) = T_i \quad (3)$$

(This is the semi-infinite slab approximation.)

3. The local heat-transfer coefficient,  $h$ , is constant with time, and the heat flux leaving the gas at the surface equals the heat flux into the model,

$$k \frac{\partial T(0,t)}{\partial x} = h[T_{aw} - T(0,t)] \quad (4)$$

where  $T_{aw}$  is the adiabatic wall temperature.

4. The model properties do not vary significantly with temperature, so that the thermal diffusivity,  $\alpha = k/\rho C_p$ , is constant with time.

5. The phase-change paint coating is very thin, so that it and the model surface are assumed to be at the same temperature at the same time,

$$T(0,t) = T_m \quad (5)$$

where  $T_m$  is the rated temperature at which the coating melts.

Based on the above assumptions, the solution (Ref. (6)) of Equation (1) may be expressed as

$$\bar{T} = 1 - e^{\beta^2} \operatorname{erfc} \beta \quad (6)$$

where  $\bar{T}$  and  $\beta$  are dimensionless parameters defined to be

$$\bar{T} = \frac{T_m - T_i}{T_{aw} - T_i} \quad (7)$$

and

$$\beta = \frac{h}{\sqrt{\rho C_p k}} \sqrt{t} \quad (8)$$

and  $\operatorname{erfc} \beta$  is the complementary error function of  $\beta$ . Equation (6) is shown graphically in Figure 1. Additional details of the solution of Equation (1) are included in Appendix B.

#### EXPERIMENTAL TECHNIQUE

##### CHOICE OF MODEL MATERIAL

From inspection of Equations (6) and (8), it is apparent that the data reduction is very sensitive to the thermophysical properties of the model. Teflon has proved to be a suitable model material for a number of reasons:

1. It is homogeneous with known thermal properties. The generally accepted thermophysical properties of Teflon are listed in Table 1.

2. It can withstand relatively high temperatures.

3. Teflon has a low thermal diffusivity. Lateral conduction effects are minimized. Thermal diffusion times,  $t_d$ , are large, thus permitting adequate test times, the criterion being that the test time (the time required for the coating to melt) must be less than the thermal diffusion time in order that the model behave like a semi-infinite slab. The restriction on the thermal diffusion time, that is, the time for a heat pulse to reach a given depth in a material, in order for the semi-infinite slab approximation to hold is given by the dimensionless parameter

$$\frac{\alpha t_d}{l^2} \leq 0.2 \quad (9)$$

(6) Carslaw, H. S., and Jaeger, J. C., Conduction of Heat in Solids, Second edition, Oxford Univ. Press, Inc., 1959, p. 71

where  $\alpha$  is the thermal diffusivity and  $\ell$  is a characteristic length, which is typically the model wall thickness. Under the restriction of Equation (9) the solutions for the finite slab and semi-infinite slab do not differ by more than 10 percent (Ref. (1)). Recently, a number of reports have provided information on how to make corrections for thin-slab, i.e., finite slab, conditions, (7,8,9) when such corrections are deemed necessary. The characteristic length in Equation (9) may well be a radius of curvature,  $R_c$ . Based on solutions in the literature (10) for constant heat flux to a surface, the difference in heat-transfer coefficient for a slab and cylinder does not exceed 10 percent when

$$\frac{\alpha t_d}{R_c^2} < 0.12 \quad ; \quad (10)$$

thus, for this limiting condition, no curvature correction is needed. As pointed out in Reference (7), Equation (10) is only rarely a more restrictive condition than Equation (9), except in a leading-edge region.

4. Teflon is sufficiently strong to withstand loading from rapid injection into the airstream (by means of a hydraulic ram, for example).

5. Teflon is impervious to the paint coating and thinner used in the tests.

The above factors support the use of Teflon as a model material in phase-change paint heat-transfer tests. The conclusion of Schultz in Reference (11) is considered to be overly harsh in excluding Teflon as a suitable material for this technique. The

- 
- (7) Maise, G., and Rossi, M. J., "Lateral Conduction Effects on Heat-Transfer Data Obtained with the Phase-Change Paint Technique," NASA-CR-2435, Aug 1974
- (8) Hunt, J. L., and Pitts, J. I., "Thin Wing Corrections of Phase-Change Heat-Transfer Data," J. Spacecraft, Vol. 8, 1971, pp. 1228-1230
- (9) Hunt, J. L., Pitts, J. I., and Richie, C. B., "Application of Phase-Change Technique to Thin-Sections with Heating on Both Surfaces," NASA TN D-7193, Aug 1973
- (10) Eckert, E. R. G., and Drake, R. M., Heat and Mass Transfer, Second edition, McGraw-Hill, New York, 1959
- (11) Schultz, H. D., "Experimental and Analytical Investigation of Temperature Sensitive Paints," AFFDL-TR-72-52, Jun 1972

apparent problem of a fluctuation in  $C_p$  around 90°F may be avoided by raising the initial temperature,  $T_i$ , of the model.

#### MODEL CONFIGURATION FOR FIN-BODY INTERFERENCE HEATING TESTS

A fin-body model was constructed using an existing five-degree half-angle cone model made of white Teflon. A conical extension of the same cone angle was fabricated from dark gray Teflon. This extension was outfitted with two cylindrically blunted fins 180° apart, one unswept and one swept 60° with respect to the cone surface normal. The fins were also made of dark gray Teflon. The cone had a stainless steel nosetip to assure a sharp tip and the fins had stainless steel shaft inserts for strength. A photograph of the model is shown in Figure 2, accompanied by a schematic diagram of the model in Figure 3. The extension is shown schematically in Figure 4. Dark gray Teflon was used for the fin-cone extension because it provided better color contrast between the model surface and the phase-change coatings, most of which dry to a light opaque color. The extension was instrumented with four embedded thermocouples, as indicated in Figure 4. These served two purposes. First, they indicated the initial temperature of the model, which is a necessary input parameter in the data-reduction scheme (see Eq. (7)). Secondly, they recorded any temperature rise at their embedded depth in the model resulting from thermal diffusion of surface heat transfer, indicative that the model was no longer behaving thermally as a semi-infinite slab.

#### PHASE-CHANGE COATINGS

Tempilaq coatings with melt temperatures of 163°F, 213°F and 263°F were selected for use in most of these tests based on estimates of aeroheating temperatures. The paints are available over the range 100°F to 2500°F in varying increments of three degrees at the lower temperatures and 50 degrees at the higher ones. The color contrast with the model and the crystalline nature of the dried coatings were also factors in these choices.

The selected paints were thinned (using a special thinner manufactured by Tempilaq) and applied to the model by means of an airbrush. Careful use of an airbrush permits one to obtain a thin, fairly uniform coating. Only a very thin coating (less than 1 mil) is needed, the assumption being that it and the surface are at the same temperature at the same time (Eq. (5)). Too heavy a coating may result in running of the coating as it melts. In addition, too thick a coating could introduce error due to latent heat of melting which is not accounted for in the theory.

#### DATA ACQUISITION

The raw data from these tests consisted of color 16mm motion pictures of the progressions of the melt lines of the Tempilaq coatings as the result of aerodynamic interference heating. The model was lightly spray-coated using an airbrush and allowed to dry. When desired flow conditions had been established in the test section of the tunnel, the movie cameras were activated as the model

was injected rapidly into the flow using the hydraulic ram facility of the NSWC/WOL Hypersonic Tunnel. Details of the tunnel facility are available in Reference (12). The model remained in the flow for test times of typically 10-20 seconds and was then retracted. Color movies of the melt line progressions were taken from top and side views using two Kodak Cine Special II cameras and Kodak 16mm Ektachrome Type EF 7241 film. The setup is shown schematically in Figure 5. Movies were taken typically at 24 frames per second.

#### PHOTOGRAPHIC CONDITIONS

A number of considerations are involved in obtaining good photographic data in this paint technique. The use of stroboscopic lighting is recommended to eliminate extraneous heating of the coatings from incandescent lamps. Radiant heat from photo floodlights can produce considerable error in the determination of the heat-transfer coefficient,  $h$ . This error may be especially significant for the lower rated coatings in the 100-150°F melting temperature range. In these tests strobe lights were mounted flush on the outside of the tunnel windows to cut down reflections and scattering of the incident light by the windows. Fairly uniform lighting of the model was achieved. There was no illumination other than that provided by these strobe lights, which were synchronized with the framing rates of the cameras.

### EXPERIMENTAL RESULTS

#### DATA REDUCTION

Values of heat-transfer coefficient,  $h$ , were obtained for various fin-cone configurations by the somewhat standard data-reduction technique for this method (1). The 16mm color movies were projected on grid paper at a convenient geometric scale which preserved the clarity of the melt lines. A stop-action projector was used, and successive locations of melt-line contours were drawn on the grid model. For a given contour the frame number was recorded, from which a melt time was deduced based on the camera framing rate and the time of initial exposure of the model to the flow. Errors in  $h$  due to uncertainties in both of these factors are discussed in a later section of this report.

#### ISOHEATING CONTOURS

Examples of the reduced heat-transfer data in the forms of lines of constant heat-transfer coefficient, so-called isoheating contours, are shown in Figures 6 through 9. Figures 6 and 7 show side and top views, respectively, of a flush-mounted unswept fin, while Figures 8 and 9 show similar data for a flush-mounted 60°-swept fin. Discussions of various aspects of the aerodynamic interference heating patterns are left to Reference (4). This report concentrates on various features of the experimental method itself. Inspection of

(12) Baltakis, F. P., "Performance Capability of the NOL Hypersonic Tunnel," NOLTR 68-187, Oct 1968

Figures 6-9 shows one advantage of the method to be that, in effect, the entire area of interest is "instrumented." Thus, a quantitative measure of heat transfer is obtained for almost all of the interference flow field. This is a recognized advantage of thermal mapping techniques, in general. One may choose to utilize these data in selecting judicious locations for discrete sensors in complementary or follow-up tests. The phase-change paint method determines both the severity and extent of the interference heating and identifies regions of extreme gradients that might have been missed by thermocouples or heat-flux gages.

#### UNCERTAINTY IN HEAT-TRANSFER COEFFICIENT

##### VALIDITY OF SEMI-INFINITE SLAB ASSUMPTION

The determined value of heat-transfer coefficient is subject to uncertainty due to uncertainties in the numerous input parameters involved in both the experimental and analytical parts of the phase-change paint method. Of primary importance is the premise that the model behave like a semi-infinite slab for the duration of a test run. This condition, that is, that the test time be less than the thermal diffusion time, is satisfied if Equation (9) is satisfied. For a Teflon model of 0.25-inch wall thickness with thermophysical properties as in Table 1, the thermal diffusion time is about 80 seconds. On areas of the model where curvature effects come into play, Equation (10) is applicable. The leading edges of the fins provide the most severe restriction, for which the thermal diffusion time is about 20 seconds. The maximum exposure times of the model in the flow were generally about 20 seconds, so in all cases the test times for which data are shown were less than the thermal diffusion time for the Teflon model. The two embedded thermocouples in the cone ahead of the fins showed no temperature rise from  $T_i$  during a run. The thermocouples embedded in the fins exhibited gradual temperature rise, especially at higher Reynolds numbers. This indicated that sides of the fins did not behave like a semi-infinite slab for the duration of a run. Consequently, the fin side-heating data are not considered to be as reliable for two higher Reynolds numbers included in Reference (4).

##### SENSITIVITY TO ERROR IN THERMOPHYSICAL PROPERTIES AND INITIAL TIME

Overall uncertainty in  $h$  is the result of uncertainty in the thermophysical properties of the model material, uncertainty in time of initial exposure to the flow, and uncertainty in the temperatures  $T_i$ ,  $T_{aw}$  and  $T_m$ . Recall Equation (8), given by

$$\beta = \frac{h}{\sqrt{\rho C_p k}} \sqrt{t} \quad , \quad (8)$$

from which

$$h = \frac{\sqrt{\rho C_p k}}{\sqrt{t}} \beta \quad . \quad (11)$$



It follows that

$$\frac{\Delta h}{h} = \frac{1}{2} \left\{ \frac{\Delta \rho}{\rho} + \frac{\Delta C_p}{C_p} + \frac{\Delta k}{k} - \frac{\Delta t}{t} \right\} + \frac{\Delta \beta}{\beta} \quad (12)$$

With respect to the first three terms on the right-hand side of Equation (12), the estimated accuracies<sup>(1,11,13)</sup> for the properties of Teflon are: density  $\rho$ , one percent; thermal conductivity  $k$ , seven percent; and specific heat  $C_p$ , five percent.

To investigate the error produced in  $h$  by uncertainty in time of initial exposure to the flow for constant properties, consider Figure 10, which shows  $\Delta h/h$  versus exposure time,  $t$ , to flow, with uncertainty in time,  $\Delta t$ , a parameter. For increasing exposure times the effect of uncertainty in initial time,  $t_0$ , decreases. For these tests  $\Delta t$  was estimated to be about 0.2 second, during which time the model passed through the core flow boundary layer. Data based on model exposure times greater than 2 seconds should be used in order to minimize  $\Delta t$  effects, as indicated in Figure 10.

#### SENSITIVITY TO ERRORS IN TEMPERATURE INPUTS

With regard to the  $\Delta \beta/\beta$  term in Equation (12), one method of attack is to estimate uncertainties in the three temperatures ( $T_i$ ,  $T_{aw}$ , and  $T_m$ ) and then to calculate  $\Delta \beta/\beta$ . Examples of such an approach may be found in Reference (14). This method is not pursued here. Instead, analytic relations have been worked out which show what relative uncertainty is produced in  $h$  for a given uncertainty in an input temperature. In each expression two temperatures are considered known and constant, while the third is allowed to vary. The three relationships were obtained by differentiating Equation (6) with respect to the varying temperature. (These expressions are not known to have appeared in the literature. An attempt at one such relationship (Ref. (15)) is considered incorrect by an inverted term and an incorrect sign.) The three equations are given by:

- (13) Kaufman, L. G., II, Ling, J., and Johnson, A. R., "Exploratory Tests Using Temperature-Sensitive Paints to Obtain Hypersonic Heat Transfer Data on Spheres and on Fin-Plate Models," GAC RM-487, Grumman Aerospace Corp., Sep 1970
- (14) Woods, J., Jr., and Carlson, J. H., "Application of Temperature Sensitive Paints for Aerodynamic Heating Analysis," MDC A1419, McDonnell Douglas Corp., Nov 1971
- (15) Edney, B. E., Bramlette, T. T., Ives, J., Hains, F. D., and Keyes, J. W., "Theoretical and Experimental Studies of Shock Interference Heating," Report No. 9500-920-195, Bell Aerospace Co., Oct 1970

$$\frac{\Delta h}{h} = \frac{\Delta T_{aw}}{T_{aw}} \frac{1}{(1 - T_i/T_{aw})} \bar{T} \Gamma(\beta) \quad , \quad (13)$$

$$\frac{\Delta h}{h} = \frac{\Delta T_i}{T_i} \frac{1}{(1 - T_i/T_{aw})} \left( \frac{T_i}{T_{aw}} \right) (1 - \bar{T}) \Gamma(\beta) \quad , \quad (14)$$

and

$$\frac{\Delta h}{h} = \frac{\Delta T_m}{T_m} \frac{(-1)}{(1 - T_i/T_{aw})} \left( \frac{T_m}{T_{aw}} \right) \Gamma(\beta) \quad , \quad (15)$$

where a common factor  $\Gamma(\beta)$  is defined as

$$\Gamma(\beta) \equiv \frac{\sqrt{\pi}}{2\beta} \frac{1}{\left[ \beta \sqrt{\pi} e^{\beta^2} \operatorname{erfc} \beta - 1 \right]} \quad . \quad (16)$$

#### SENSITIVITY TO ERROR IN ADIABATIC WALL TEMPERATURE

Equation (13) shows that error in  $h$  due to error in  $T_{aw}$  is proportional to  $\bar{T}$ . Thus, error in  $h$  may be minimized by choosing test conditions with small  $\bar{T}$ , where  $\bar{T}$  is defined in Equation (7). In addition, test conditions with small  $(T_i/T_{aw})$  help minimize error in  $h$ . This small  $(T_i/T_{aw})$  condition is advantageous in all three equations. The  $(1 - T_i/T_{aw})$  factor in the denominator was purposely not included in the definition of  $\Gamma(\beta)$  in order to emphasize the importance of low  $(T_i/T_{aw})$  ratio. Figure 11 shows Equation (13) for three different values of  $T_m$  for  $T_i/T_{aw} = 0.7$ . These values are typical of conditions for the results shown in Figures 6-9 and in Reference (4).

#### SENSITIVITY TO ERROR IN INITIAL MODEL TEMPERATURE

Equation (14) demonstrates that the error in  $h$  varies as  $(1 - \bar{T})$  with error in initial temperature,  $T_i$ , where once again the initial temperature to recovery temperature is an important factor. Here it is doubly important to keep the ratio  $(T_i/T_{aw})$  small, the effect being a combined one of  $(T_i/T_{aw})$  in the numerator and  $[1 - (T_i/T_{aw})]$  in the denominator. Figure 12 shows Equation (14) for three different values of  $T_m$ .

#### SENSITIVITY TO ERROR IN MELT TEMPERATURE OF PHASE-CHANGE COATING

The last relationship, Equation (15), specifies what uncertainty in  $h$  results from uncertainty in melt temperature,  $T_m$ , of the paint. This error in  $h$  is proportional to the ratio  $(T_m/T_{aw})$  and again

varies inversely with the  $(1 - T_i/T_{aw})$  factor. Equation (15) is shown in Figure 13 for several different paint-melt temperatures.

#### GENERAL COMMENTS

The analytic expressions in Equation (13)-(15) should provide guidelines for the design of experiments using the phase-change paint technique in order to minimize uncertainty in the  $h$  values.

Based on all the uncertainties in input temperatures, time, and Teflon properties, most of the  $h$  values shown in Figures 6-9 appear to be good within about 20 percent.

The extreme sensitivity of error in  $h$  due to uncertainties in  $T_i$  or  $T_m$  in Figures 12 and 13, respectively, reflect the fact that the solution to the heat-conduction equation is very sensitive to its boundary conditions, which themselves predicate knowledge of  $T_i$  and  $T_m$ . Initial temperature,  $T_i$ , is generally known within one percent from thermocouple data, and coating melt temperature,  $T_m$ , is frequently known within one percent (see Appendix A). Again, the uncertainty in  $h$  goes inversely as  $(1 - T_i/T_{aw})$ , so a small  $(T_i/T_{aw})$  ratio is always desirable.

#### CONCLUSIONS

A marked advantage of the phase-change paint method is that, in effect, the entire area of interest on the model is instrumented. In addition, models generally may be fabricated faster and at a lower cost than, for example, thin-walled models. Even if flow conditions in a given facility do not allow one to determine  $h$  values with low relative uncertainty per Equations (13)-(15), it is still possible to conduct a relatively inexpensive initial test using paints to help determine placement locations for discrete sensors for follow-up tests.

One disadvantage of the method is a problem associated with most optical methods, namely, the tedious reduction of the photographic (movie) data to visually identify the melt-line locations. This identification may vary somewhat with the observer and with the clarity of the film record. In addition, camera angle and model attitude must be accounted for if one wishes to obtain careful spatial distributions of  $h$  over the model surface in the form of  $h$  versus distance.

Overall, the phase-change paint technique is considered capable of providing reliable quantitative heat-transfer data. The technique is especially useful on complex geometries involving aerodynamic interference heating patterns of initially unknown extent and location. With careful experiment designing, based on guidelines provided here, one may expect to obtain heat-transfer measurements

NSWC/WOL/TR 75-62

from the phase-change paint method which would be just as reliable as results from other methods employing discrete sensors.

TABLE 1

## THERMOPHYSICAL PROPERTIES OF TEFLON\*

Density, lb/ft <sup>3</sup>	137.0
Specific heat, BTU/lb °R	0.25
Thermal Conductivity, BTU/sec-ft-°R	$3.89 \times 10^{-5}$
Melting Temperature, °F	~900°F
Thermal Diffusivity, ft <sup>2</sup> /sec	$1.14 \times 10^{-6}$

---

\*See References (1), (11) and (13)

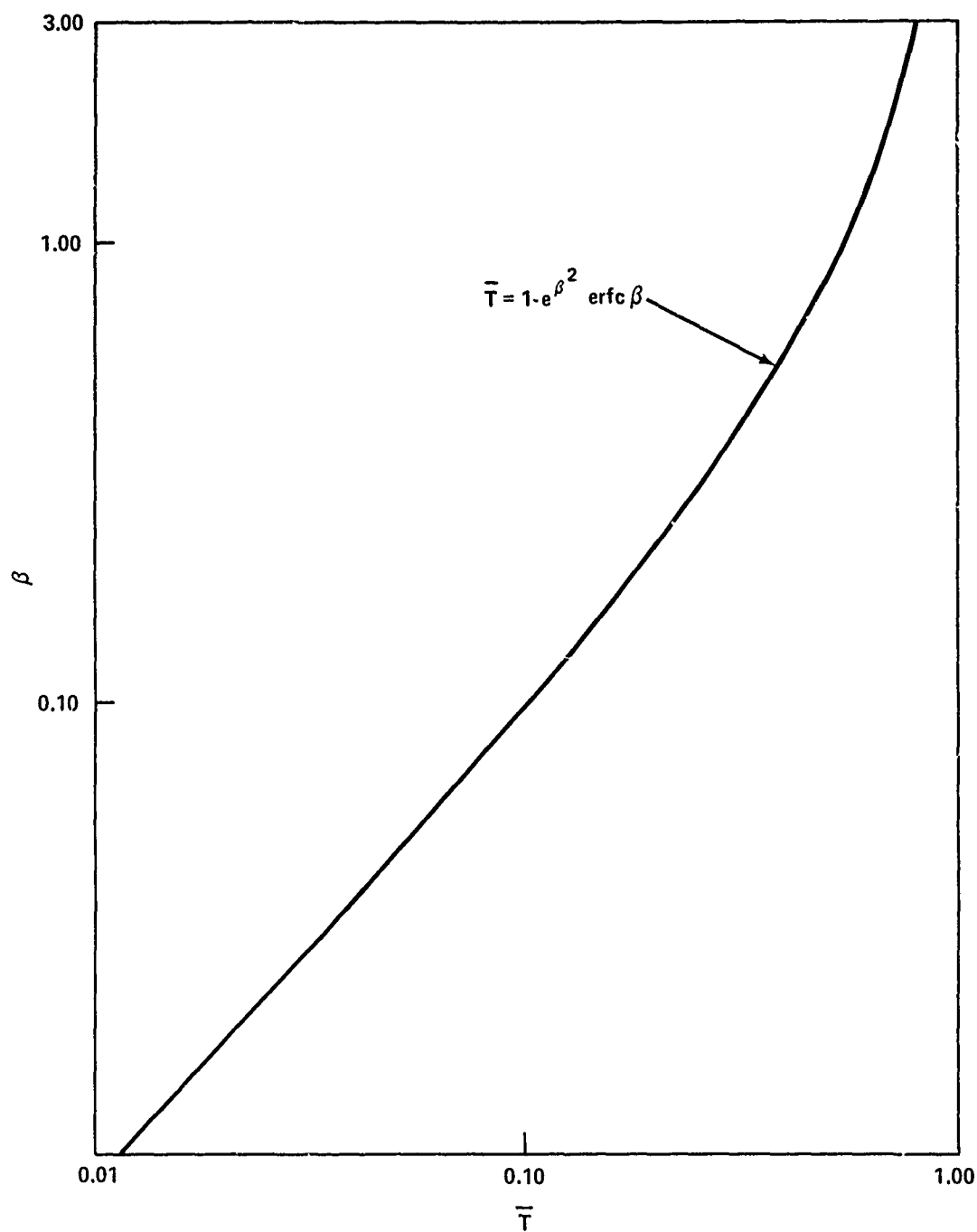


FIG. 1 SOLUTION OF ONE-DIMENSIONAL HEAT CONDUCTION EQUATION

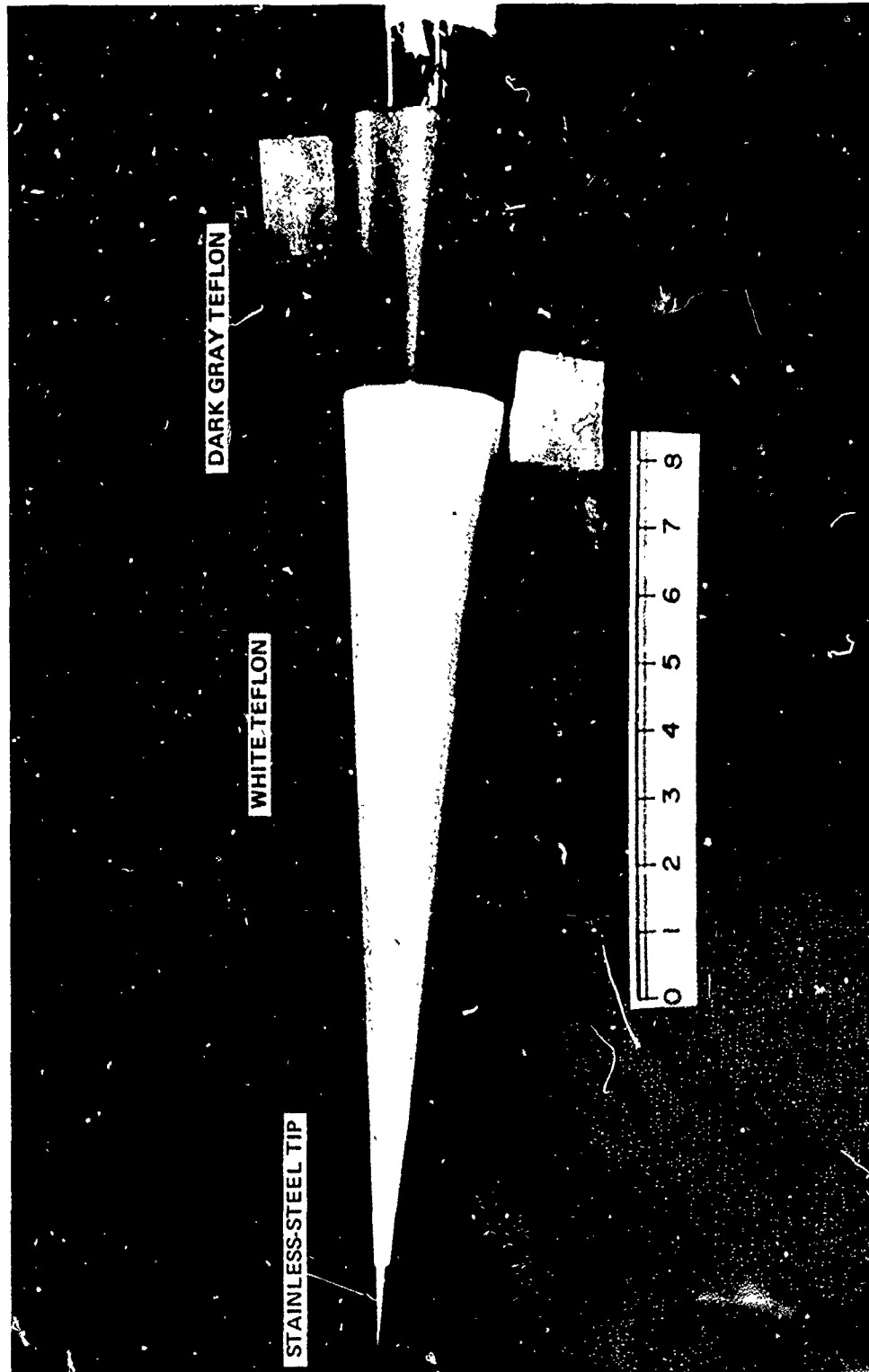


FIG. 2 TEFLON HEAT-TRANSFER MODEL (SCALE IN INCHES)

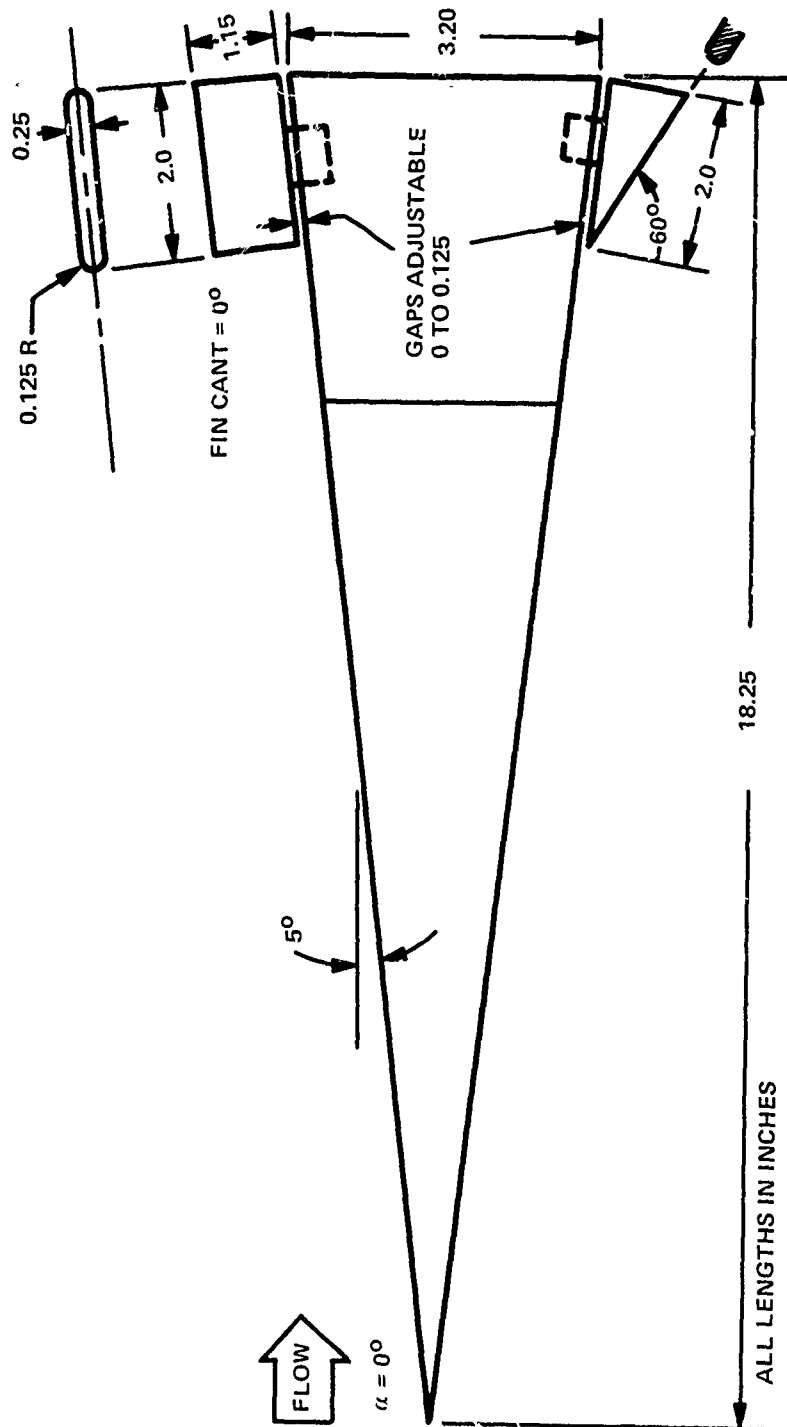


FIG. 3 SCHEMATIC DIAGRAM OF FIN-CONE MODEL



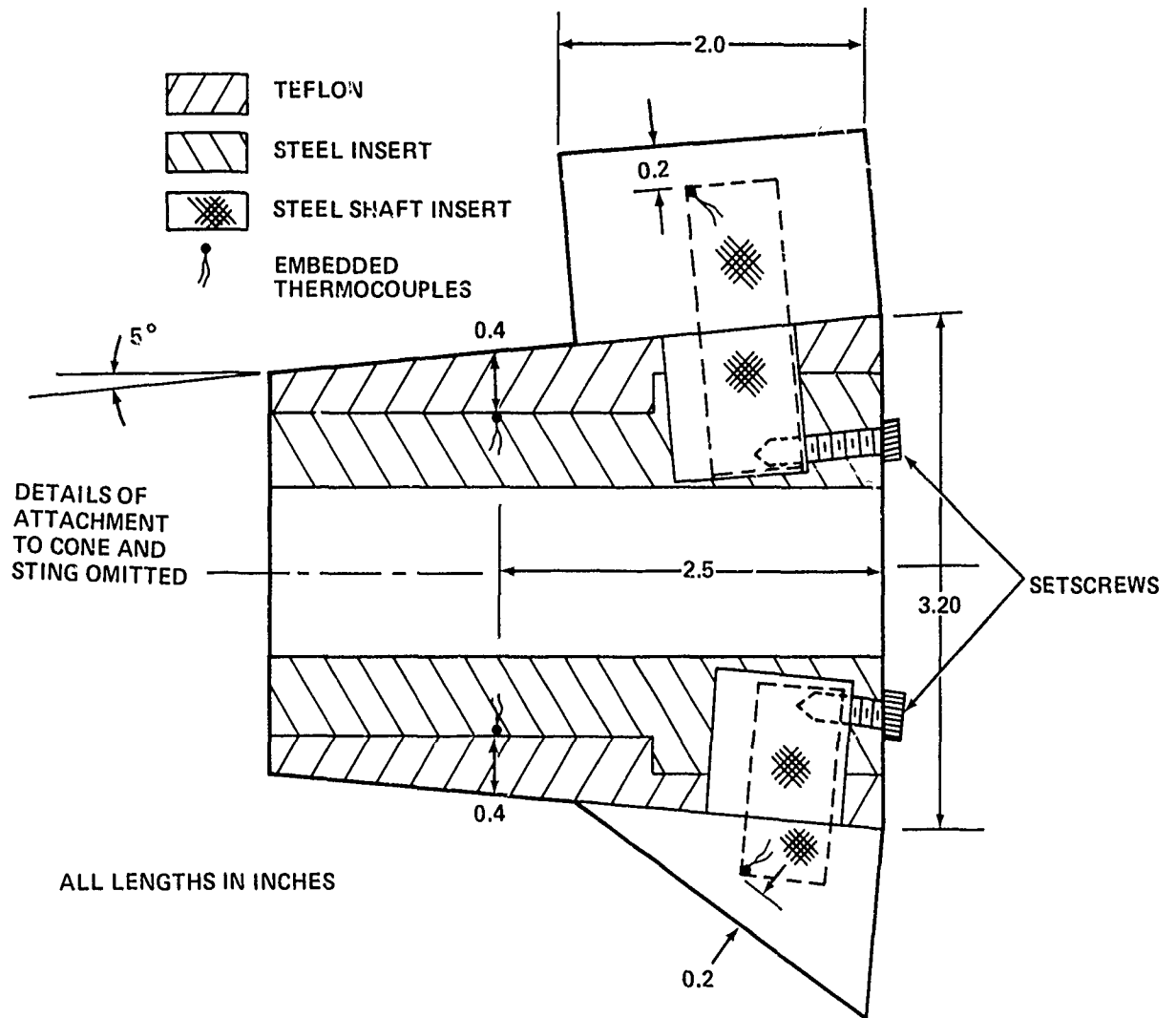


FIG. 4 SCHEMATIC DIAGRAM OF FINNED EXTENSION

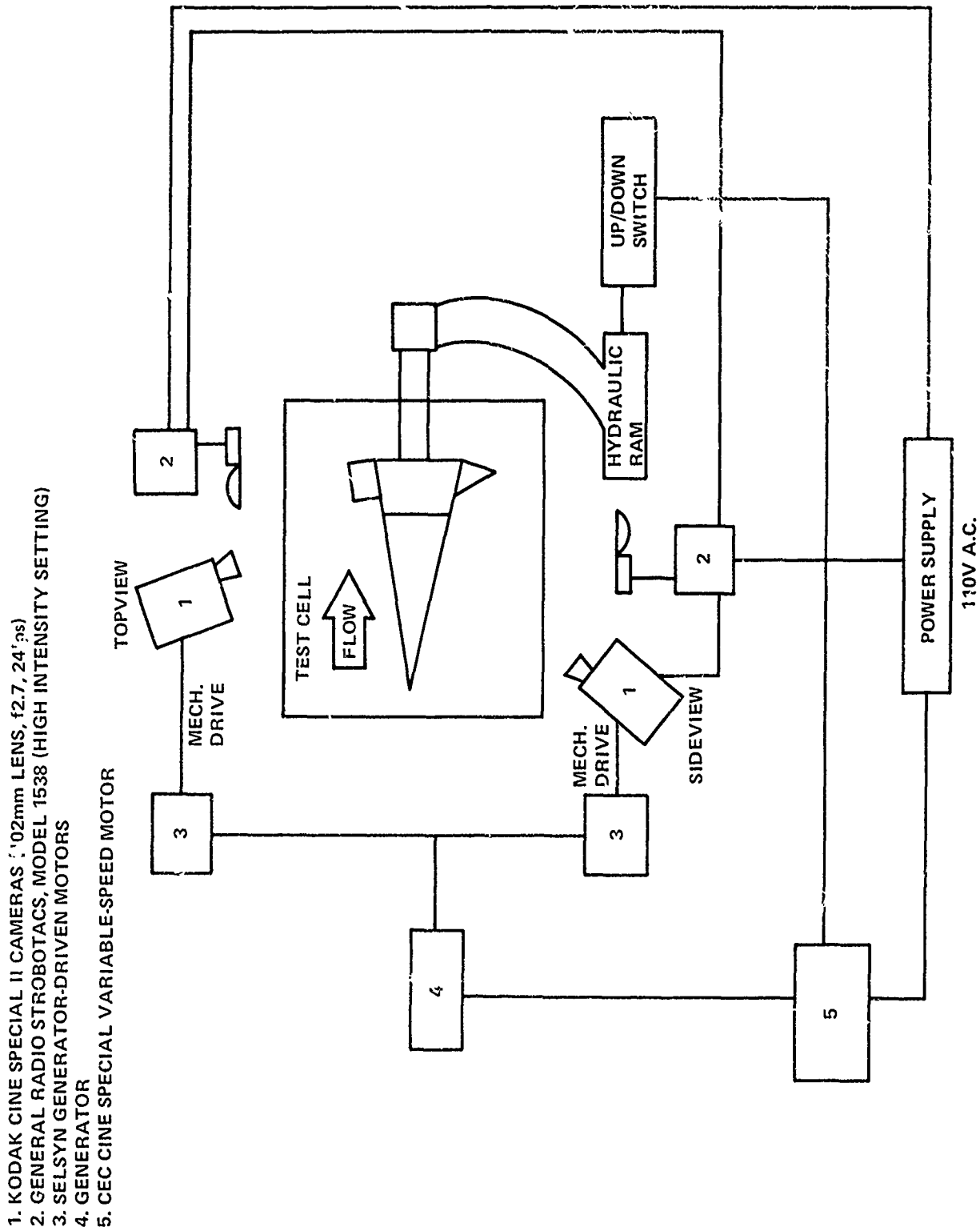


FIG. 5 SCHEMATIC DIAGRAM OF TEST SETUP

$M_\infty = 5$   
 $Re_\infty/FT = 4.5 \times 10^6$   
 GAP = 0.0"

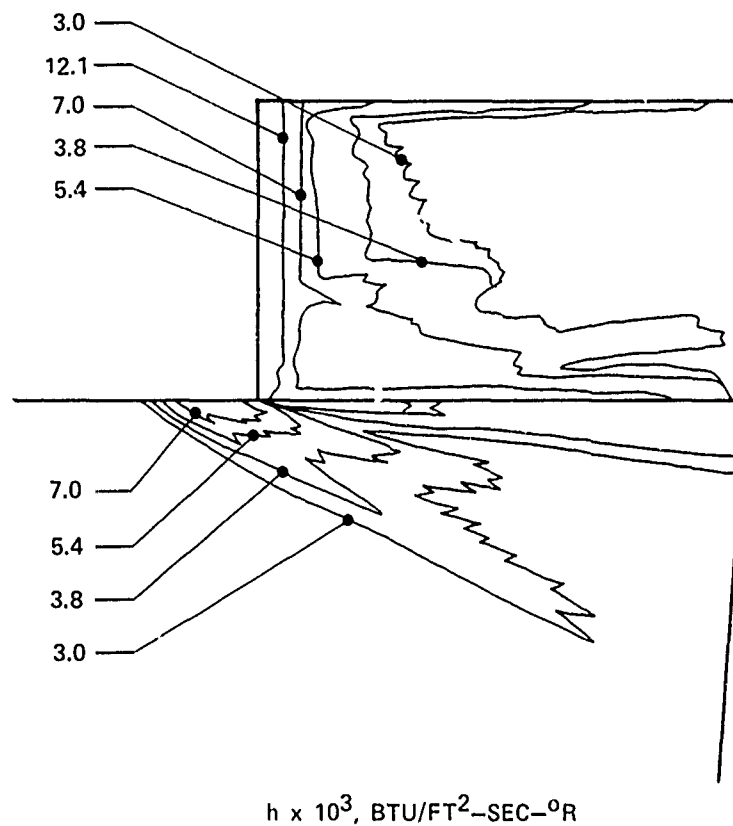


FIG. 6 ISOHEATING CONTOURS FOR FLUSH-MOUNTED  
 UNSWEPT FIN. SIDE VIEW

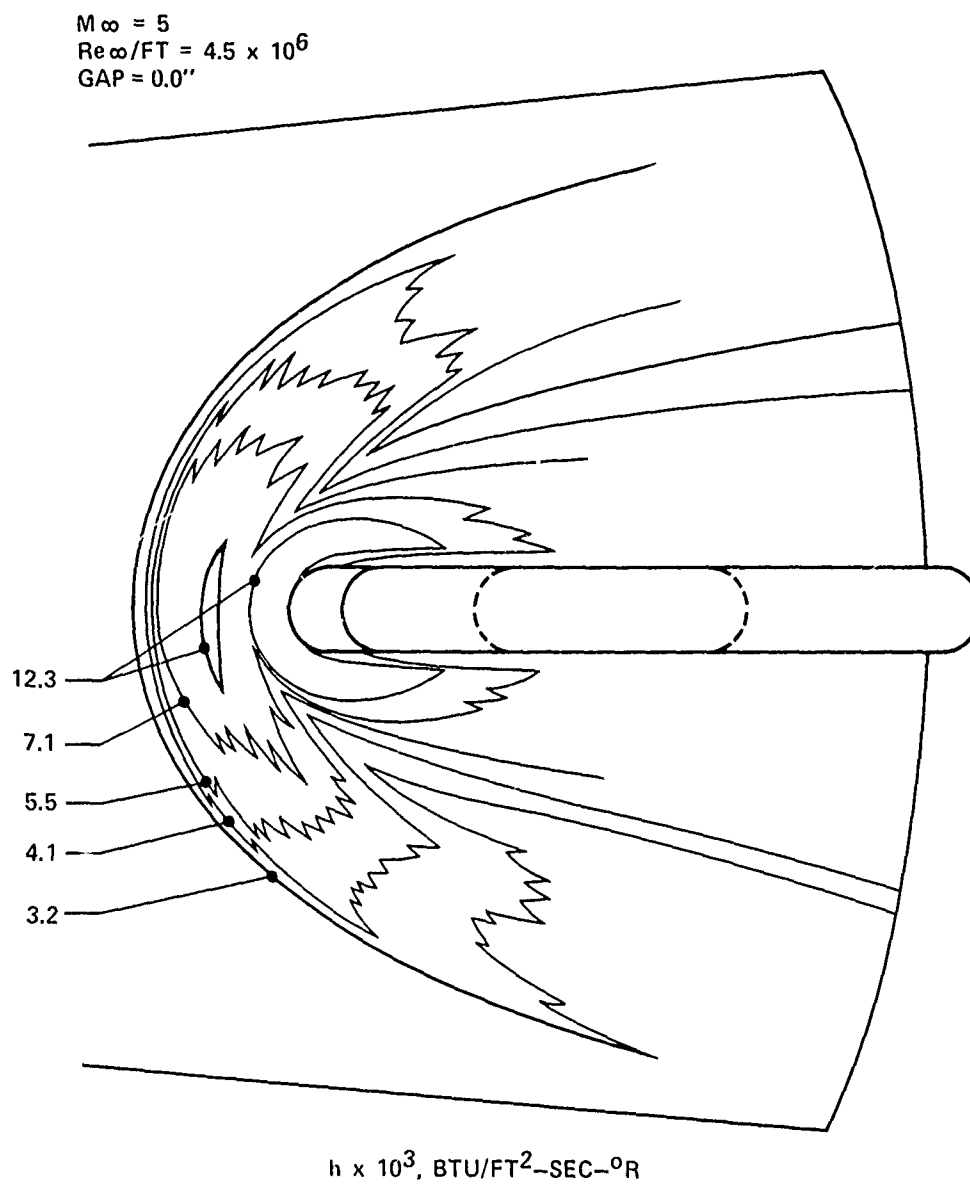


FIG. 7 ISOHEATING CONTOURS FOR FLUSH-MOUNTED UNSWEPT FIN. TOP VIEW, ABOUT  $10^{\circ}$  FORWARD OF LEADING EDGE

$M_{\infty} = 5$   
 $Re_{\infty}/FT = 4.5 \times 10^6$   
 $GAP = 0.0''$

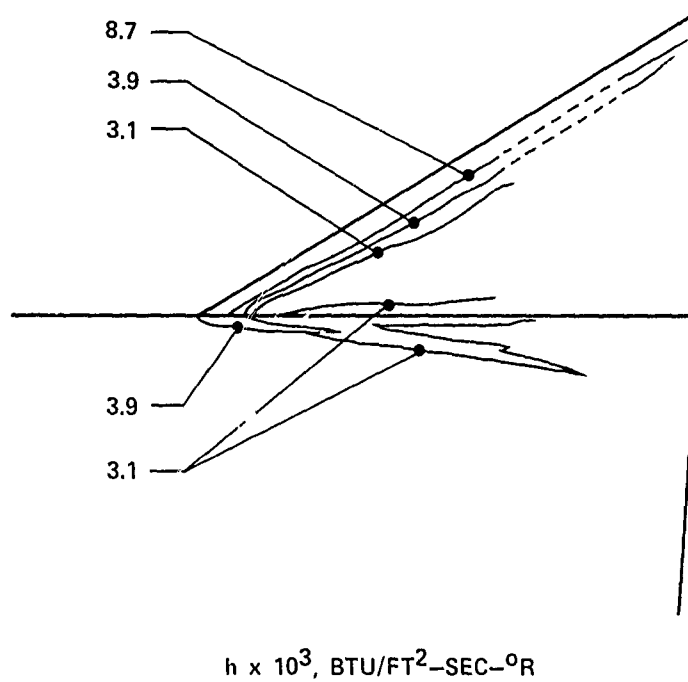


FIG. 8 ISOHEATING CONTOURS FOR FLUSH-MOUNTED 60°-SWEPT FIN. SIDE VIEW.

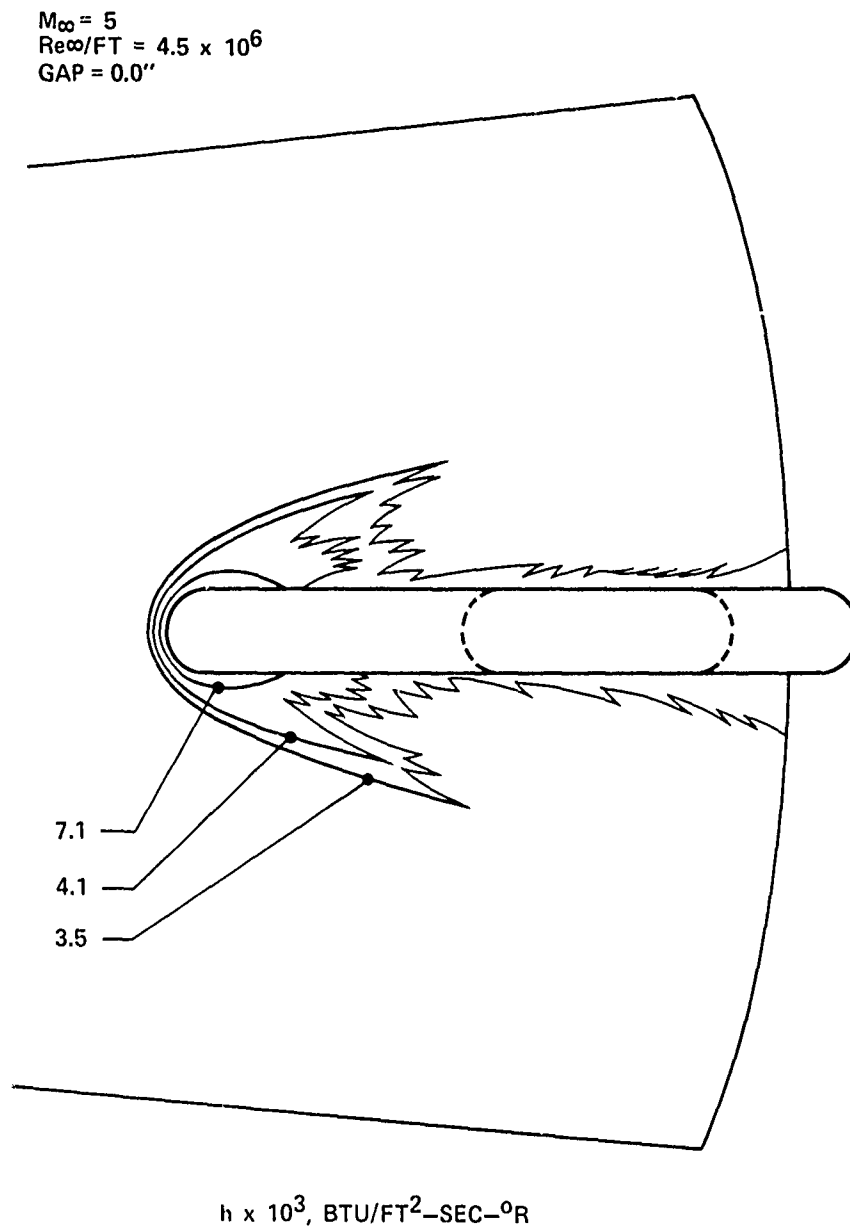


FIG. 9 ISOHEATING CONTOURS FOR FLUSH-MOUNTED 60°-SWEEP  
FIN. TOP VIEW

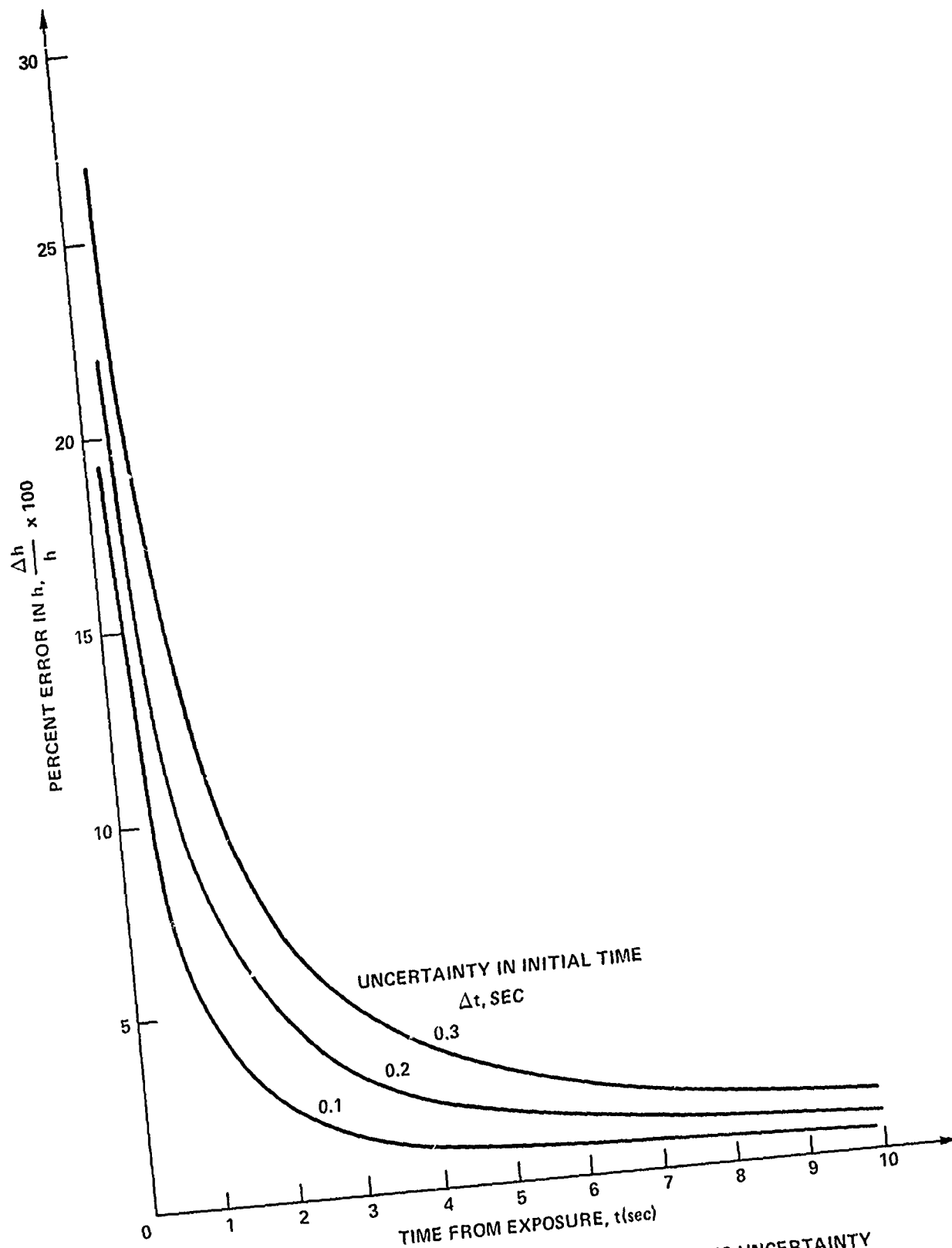


FIG. 10 ERROR IN HEAT-TRANSFER COEFFICIENT DUE TO UNCERTAINTY IN INITIAL TIME OF EXPOSURE TO FLOW

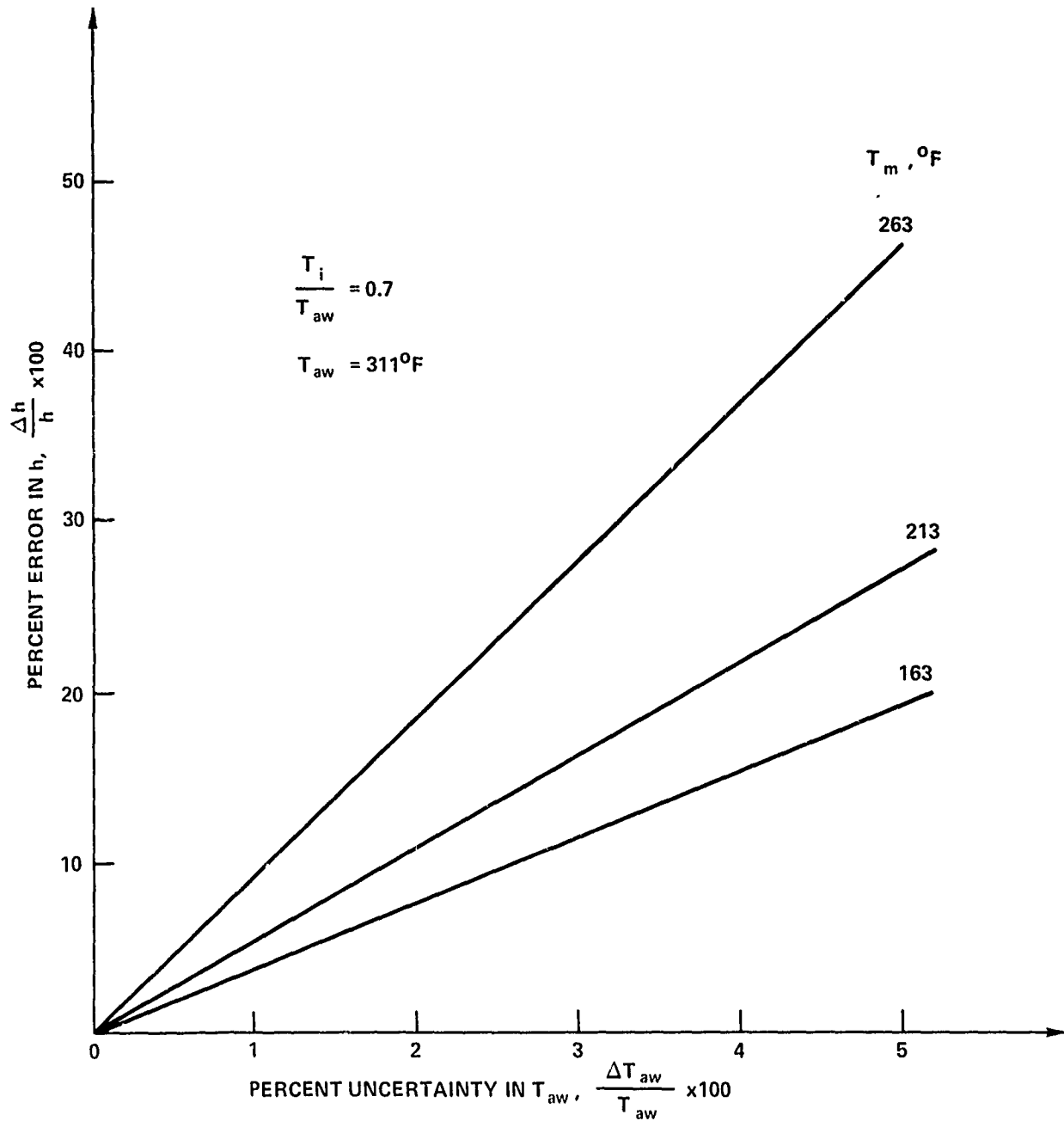


FIG. 11 ERROR IN HEAT-TRANSFER COEFFICIENT DUE TO UNCERTAINTY IN ADIABATIC WALL TEMPERATURE



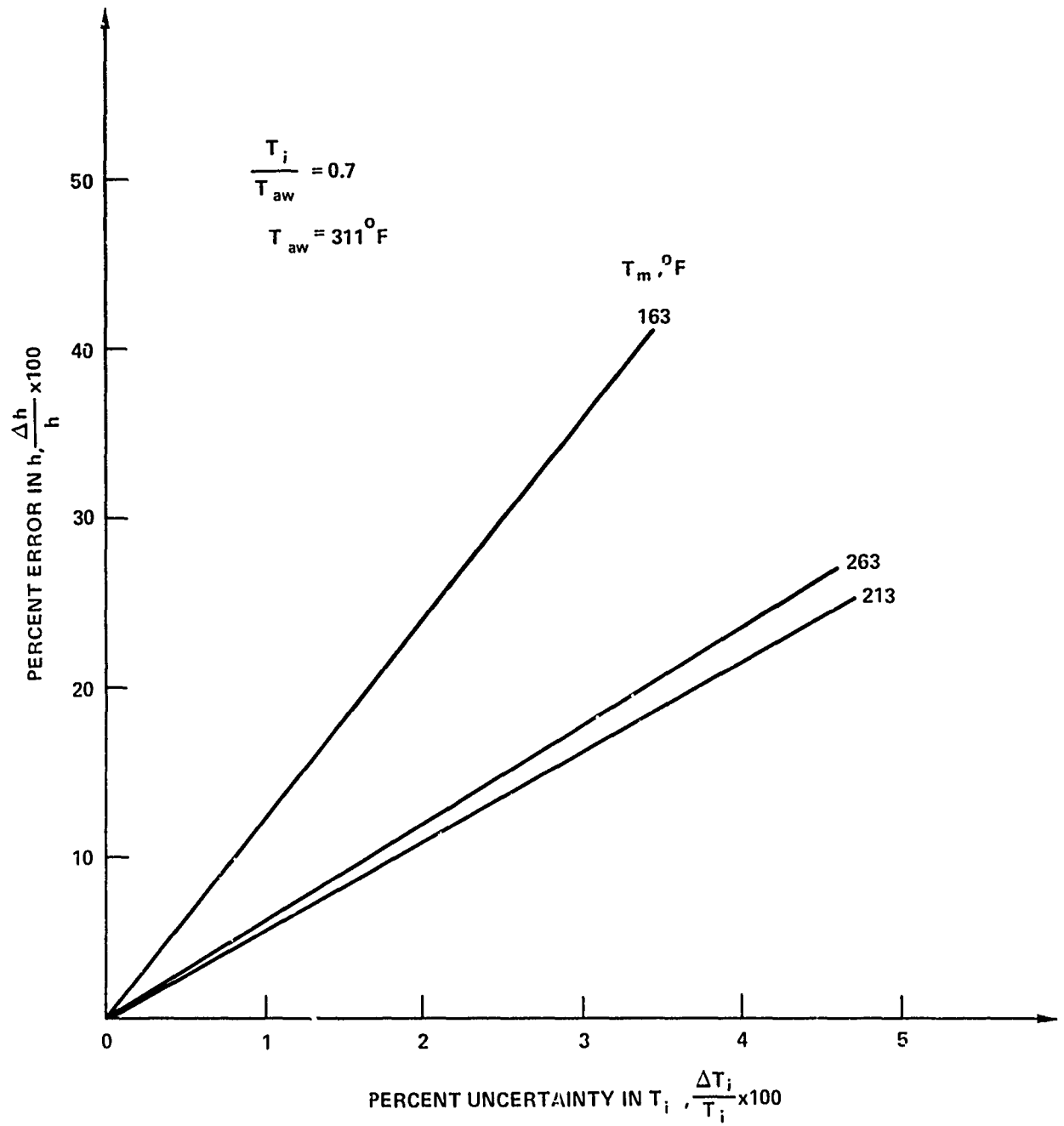


FIG. 12 ERROR IN HEAT-TRANSFER COEFFICIENT DUE TO UNCERTAINTY IN INITIAL MODEL TEMPERATURE

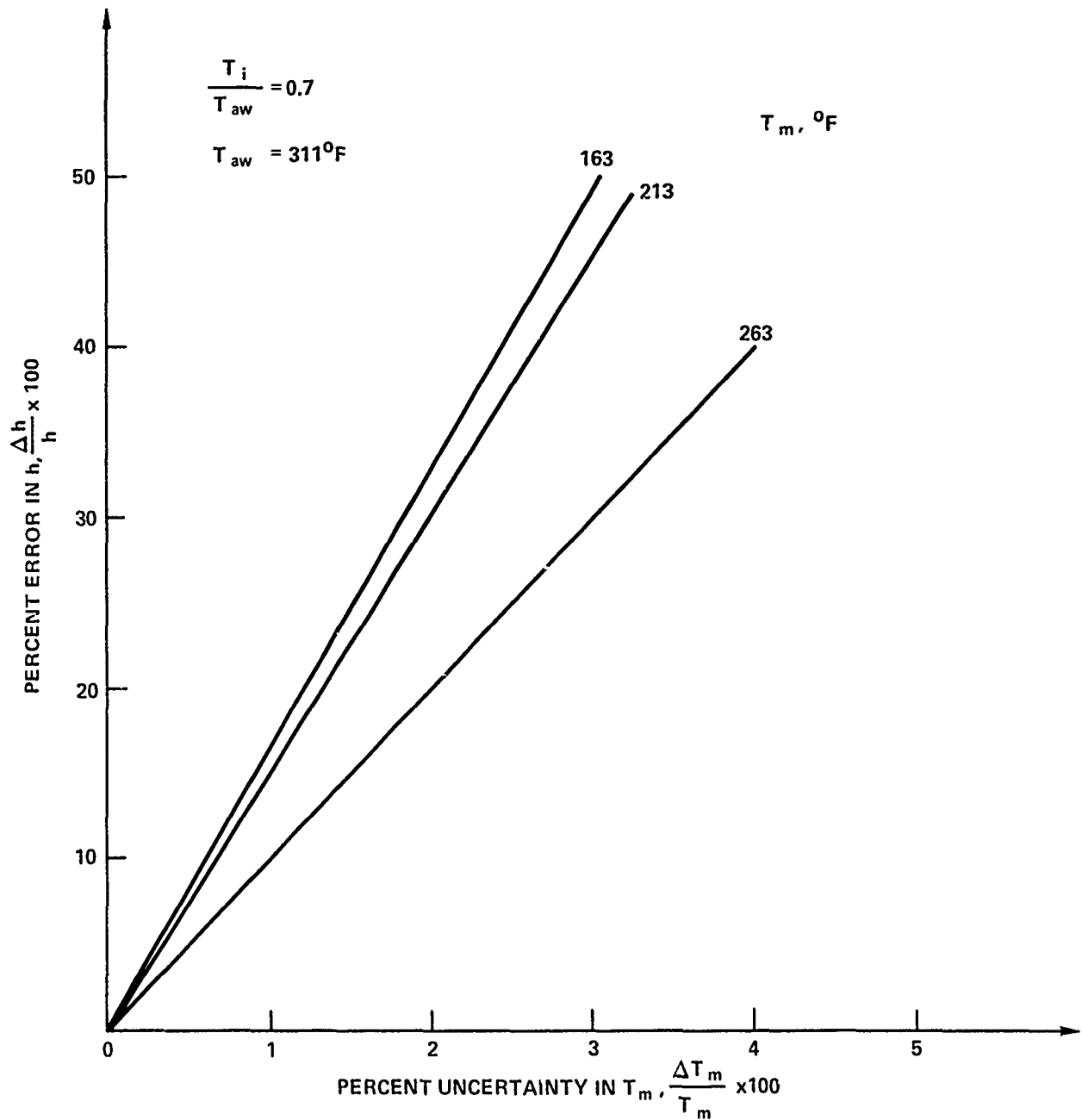


FIG. 13 ERROR IN HEAT-TRANSFER COEFFICIENT DUE TO UNCERTAINTY IN PHASE-CHANGE PAINT MELT TEMPERATURE

## APPENDIX A

## PHASE-CHANGE PAINT CALIBRATION

A schematic diagram of the calibration setup is shown in Figure A-1. The rig consisted of a single chromel-alumel thermocouple spot-welded to a 1/32-inch-thick stainless steel plate. The thermocouple output was fed through an electronic cold junction compensator into a strip recorder. The strip recorder was calibrated using a millivolt potentiometer source. The plate was heated by a heat lamp on the side opposite the thermocouple.

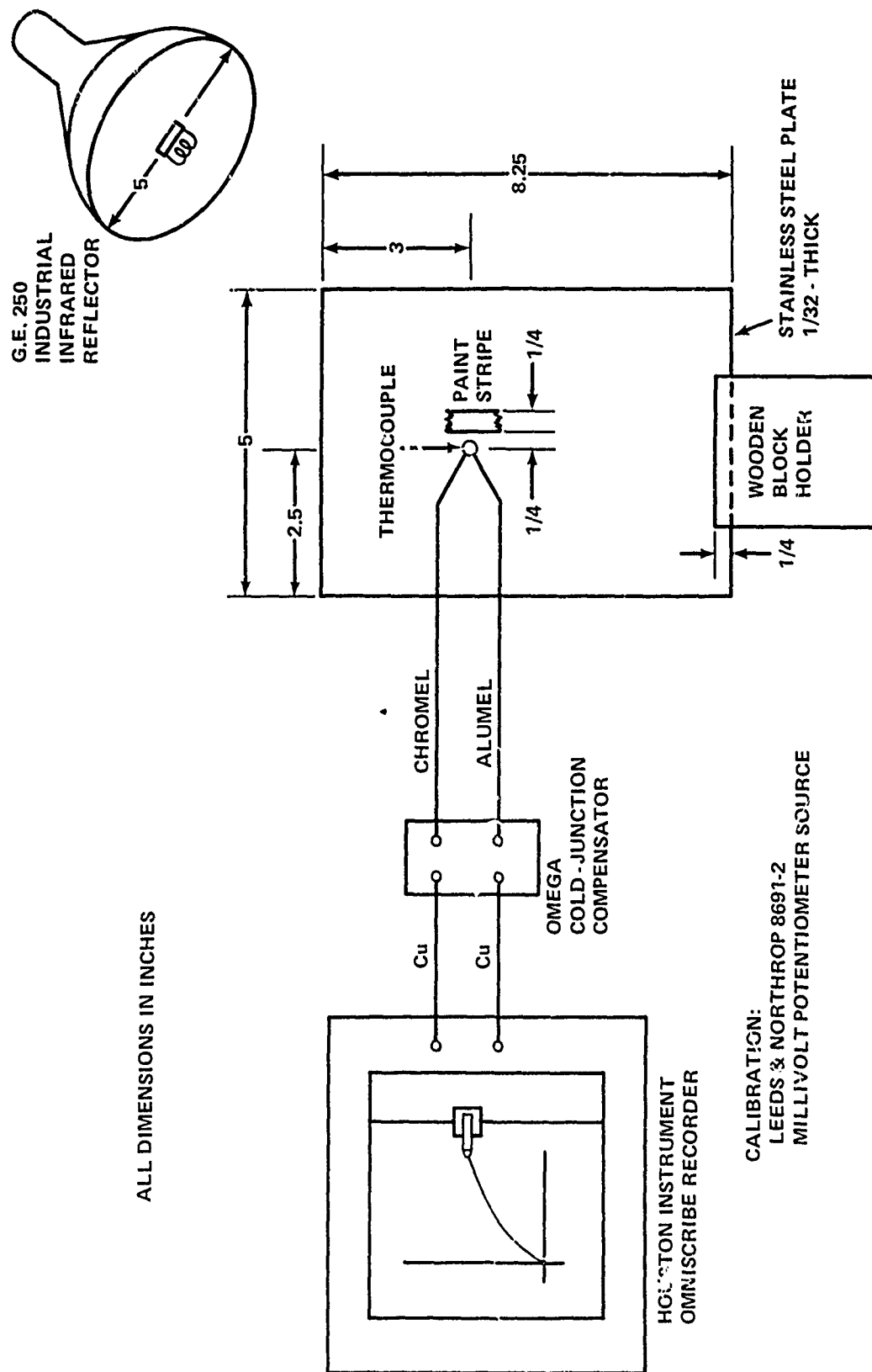
A roughly 1/2-inch by 1/4-inch strip of the paint being checked was brushed on the plate about 1/4 inch to the right of the thermocouple and allowed to dry. The heat lamp was turned on and a temperature-time history was recorded for the thermocouple. When the paint coating was observed to turn clear (melt), the scribe on the recorder was raised and released to mark the spot on the history curve. The heating rate could be varied somewhat by moving the plate relative to the heat lamp. Jones and Hunt(1) found almost no variation of melt temperature with either pressure or heating rate for Tempilaq coatings. The calibration results for a number of paints are shown in Table A-1 for a heating rate of about 4°F/sec. The observed melting temperatures of the coatings agreed well with their rated temperatures. The manufacturer specifies Tempilaq paints to melt within  $\pm 1$  percent of their rated output. Of the nine coatings tested, five were within one percent, one was within two percent, two were within three percent and one was within four percent.

TABLE A-1  
PHASE-CHANGE PAINT CALIBRATION RESULTS

Rated Temperature (°F)	Tempilaq		Difference** (%)
	Observed Phase- Change Temperature*, (°F)	Observed Phase- Change Temperature*, (°F)	
163	172	172	3.0
206	207	207	0.5
213	221	221	1.9
250	256	256	2.4
263	269	269	0.4
294	293	293	0.3
350	364	364	4.0
388	388	388	-
450	449	449	0.2

\* Temperature rise rate was about 4°F/sec at ambient conditions of 70°F and 1 atmosphere.

\*\* | (Observed Temperature-Rated Temperature) | x 100/Rated Temperature



ALL DIMENSIONS IN INCHES

FIG. A-1 SCHEMATIC DIAGRAM OF TEMPERATURE-SENSITIVE PAINT CALIBRATION SETUP

## APPENDIX B

## GENERAL SOLUTION OF HEAT EQUATION

The one-dimensional heat-conduction equation given by Equation (1), subject to the boundary conditions in Equations (2), (3) and (4), has a general solution (Refs. (6), (16)) for temperature,  $T$ , at time,  $t$ , at any depth,  $x$ , into the semi-infinite slab given by:

$$\frac{T(x,t) - T_i}{T_{aw} - T_i} = 1 - \operatorname{erf} \left( \frac{x}{\sqrt{4\alpha t}} \right) - \exp \left( \frac{hx}{k} + \frac{h^2 \alpha t}{k^2} \right) \operatorname{erfc} \left( \frac{x}{\sqrt{4\alpha t}} + \frac{h}{k} \sqrt{\alpha t} \right) \quad (\text{B-1})$$

where  $\alpha$  is the thermal diffusivity defined as  $\alpha \equiv k/\rho C_p$ .

At the model surface,  $x = 0$  and  $T(0,t)$  is assumed to be equal to the melt temperature of the phase-change coating, so that  $T(0,t) = T_m$ . The left-hand side of Equation (B-1) becomes  $\bar{T}$  as defined by Equation (7), and the right-hand side may be simplified since  $\operatorname{erf}(0) = 0$ . Equation (B-1) becomes

$$\bar{T} = 1 - \exp \left( \frac{h^2}{k^2} \alpha t \right) \operatorname{erfc} \left( \frac{h}{k} \sqrt{\alpha t} \right) \quad (\text{B-2})$$

Recalling the definition of  $\beta$  from Equation (8), Equation (B-2) becomes

$$\bar{T} = 1 - e^{\beta^2} \operatorname{erfc} \beta,$$

in agreement with Equation (6).

(16) Slattery, J. C., "Momentum, Energy and Mass Transfer in Continua," McGraw-Hill, 1972, pp. 310-314